Chapter 5

Half-space problem

5.1 General

This chapter deals with a problem encountered in many practical applications: determine the electromagnetic field produced by a known source, when the medium comprises of uniform layers. The assumption of a layered structure makes it possible to derive analytic solutions, which is generally not the case for more complicated structures. This is just a form of scattering problems, although we will now assume infinitely large bodies contrary to the previous chapter, and the incoming field is generally not a plane wave.

The method of solution is straightforward:
1) Solve the wave equation is each layer. A typical case is that sources are within one layer ("air"), so the wave equation is nonuniform there and uniform elsewhere ("earth").
2) Apply boundary conditions to combine the solutions of the wave equation in separate layers. Typical physicality conditions are also required, for example, finite fields at infinity.

We will start with a dipole source above a layered structure (the Sommerfeld half-space problem). This is a basic model, since any source can be constructed of dipoles. It is convenient to use the Hertz vector in this connection. However, when we deal with more general sources, we will use the vector potential. As a concrete example, we will derive the analytical solution of fields due to a horizontal current system above a layered earth. After having the exact results, we will show how they can be converted in another form, which appears to be the method of images. This allows for a derivation of handy approximations of the exact formulas. We will also discuss a simple model that allows for the treatment of a two-dimensional conductivity structure with conformal mapping. As a practical example, we

will introduce investigations of geomagnetically induced currents.

5.2 Sommerfeld half-space problem

Assume that the xy-plane divides the space into two uniform parts: "air" (medium 0) and "earth" (medium 1), whose electromagnetic parameters are $(\mu_0, \epsilon_0, \sigma_0)$ and $(\mu_1, \epsilon_1, \sigma_1)$, respectively. Set a vertical dipole $\mathbf{J}(\mathbf{r}, t) = IL\delta(x)\delta(y)\delta(z-h)e^{-i\omega t}\mathbf{e}_z$ in the air at the altitude h. We use a cylindrical coordinate system (ρ, ϕ, z), where the z-axis points upwards. It is convenient to use the Hertz vector to calculate the fields. First,

$$IL\delta(x)\delta(y)\delta(z-h)e^{-i\omega t}\mathbf{e}_z = \mathbf{J} = \frac{\partial \mathbf{p}}{\partial t} + \frac{\sigma_0}{\epsilon_0}\mathbf{p} = (-i\omega + \frac{\sigma_0}{\epsilon_0})p\mathbf{e}_z e^{-i\omega t} \quad (5.1)$$

so the inhomogeneous wave equation in the air is (cf. Eq. 2.48)

$$\nabla^2\mathbf{\Pi} + k^2\mathbf{\Pi} = -\frac{1}{\epsilon_0}p\mathbf{e}_z = -\frac{IL}{\sigma_0 - i\omega\epsilon_0}\delta(x)\delta(y)\delta(z-h)\mathbf{e}_z \quad (5.2)$$

where $k^2 = \omega^2\mu_0\epsilon_0 + i\omega\mu_0\sigma_0$. It is clear that the Hertz vector has only a z component, $\mathbf{\Pi} = \Pi\mathbf{e}_z$. The solution of the inhomogeneous wave equation in the air is

$$\begin{aligned}\Pi_p = \frac{IL}{4\pi(\sigma_0 - i\omega\epsilon_0)} \int d^3\mathbf{r}' \, \frac{\delta(x')\delta(y')\delta(z'-h)e^{ik_0|\mathbf{r}-\mathbf{r}'|}}{|\mathbf{r}-\mathbf{r}'|} \\ = \frac{ILe^{ik_0 r}}{4\pi(\sigma_0 - i\omega\epsilon_0)r}\end{aligned} \quad (5.3)$$

where $r = \rho^2 + (z-h)^2$ is the distance from the dipole, and the subscript p refers to the primary field. One advantage of using the Hertz vector is obvious: although the charge density does not vanish, it does not have to be included explicitly.

The electric field is

$$\mathbf{E} = \nabla \times (\nabla \times \mathbf{\Pi}) - \frac{1}{\epsilon}\mathbf{p} = \nabla(\nabla \cdot \mathbf{\Pi}) + k^2\mathbf{\Pi} \quad (5.4)$$

which gives the components

$$E_\rho = \frac{\partial^2\Pi}{\partial\rho\partial z}, \; E_\phi = 0, \; E_z = k^2\Pi + \frac{\partial^2\Pi}{\partial^2 z} \quad (5.5)$$

The magnetic field is

$$\mathbf{B} = \mu\nabla \times (\epsilon\frac{\partial\mathbf{\Pi}}{\partial t} + \sigma\mathbf{\Pi}) \quad (5.6)$$

and in the component form

$$B_\rho = 0,\ B_\phi = -\mu(\sigma - i\omega\epsilon)\frac{\partial \Pi}{\partial \rho},\ B_z = 0 \tag{5.7}$$

It is also necessary to solve the homogeneous wave equation in the air and in the earth to get the secondary field. In the air, the total field is then the sum of the primary and secondary fields. In the earth, the total field equals to the secondary field. Due to the azimuthal symmetry, there is no ϕ dependence, so the homogeneous wave equation is

$$(\frac{1}{\rho}\frac{\partial}{\partial \rho}\rho\frac{\partial}{\partial \rho} + \frac{\partial^2}{\partial z^2})\Pi(\rho, z) + k^2\Pi(\rho, z) = 0 \tag{5.8}$$

Its well-behaving solution is $C(b)J_0(b\rho)e^{\pm K_j z}$, where b is real and the generalised wave number K is defined by

$$K_j = \sqrt{b^2 - k_j^2}\ ;\ -\pi/2 \leq arg(K_j) < \pi/2\ ;\ j = 0, 1 \tag{5.9}$$

Note especially that the phase condition implies that $K(b = 0) = -ik$ with the harmonic time dependence $e^{-i\omega t}$. In the air ($z > 0$) the acceptable exponential term is $e^{-K_0 z}$ and in the earth $e^{+K_1 z}$ to guarantee finite solutions everywhere.

Consequently, we can express the Hertz vectors in the air (0) and in the earth (1) as follows:

$$\Pi_0 = \frac{ILe^{ik_0 r}}{4\pi(\sigma_0 - i\omega\epsilon_0)r} + \frac{IL}{4\pi(\sigma_0 - i\omega\epsilon_0)}\int_0^\infty db\ \frac{bR(b)e^{-K_0 h}}{K_0}e^{-K_0 z}J_0(b\rho) \tag{5.10}$$

$$\Pi_1 = \frac{IL}{4\pi(\sigma_0 - i\omega\epsilon_0)}\int_0^\infty db\ T(b)e^{K_1 z}J_0(b\rho) \tag{5.11}$$

where the coefficients $R(b), T(b)$ will be solved from the boundary conditions. To proceed, we use the following identity:

$$\frac{e^{ik_0 r}}{r} = \int_0^\infty db\ \frac{be^{-K_0|z-h|}}{K_0}J_0(b\rho) \tag{5.12}$$

(Stratton, 1941, p. 576), when the primary Hertz vector becomes

$$\Pi_p = \frac{ILe^{ik_0 r}}{4\pi(\sigma_0 - i\omega\epsilon_0)r} = \frac{IL}{4\pi(\sigma_0 - i\omega\epsilon_0)}\int_0^\infty db\ \frac{be^{-K_0|z-h|}}{K_0}J_0(b\rho) \tag{5.13}$$

Now it is easy to apply the continuities of the tangential fields at the earth's surface (mathematically, we deal with the Fourier-Bessel transform,

see Stratton, 1941, p. 371). These conditions are satisfied if $\partial\Pi/\partial z$ and $(\sigma - i\omega\epsilon)\Pi$ are continuous. This leads to equations

$$\begin{aligned} be^{-K_0 h}(1 - R(b)) &= K_1 T(b) \\ \frac{b}{K_0}(\sigma_0 - i\omega\epsilon_0)e^{-K_0 h}(1 + R(b)) &= (\sigma_1 - i\omega\epsilon_1)T(b) \end{aligned} \tag{5.14}$$

which yields

$$\begin{aligned} R(b) &= \frac{N^2 K_0 - K_1}{N^2 K_0 + K_1} \\ T(b) &= \frac{2be^{-K_0 h}}{N^2 K_0 + K_1} \end{aligned} \tag{5.15}$$

where

$$N^2 = \frac{\sigma_1 - i\omega\epsilon_1}{\sigma_0 - i\omega\epsilon_0} \tag{5.16}$$

The total Hertz vector in the air ($z > 0$) is thus

$$\Pi = \frac{IL}{4\pi(\sigma_0 - i\omega\epsilon_0)} \int_0^\infty db\, \frac{b}{K_0}(e^{-K_0|z-h|} + \frac{N^2 K_0 - K_1}{N^2 K_0 + K_1} e^{-K_0(z+h)}) J_0(b\rho) \tag{5.17}$$

The first term in the integrand corresponds to the primary field and the second one to the secondary field, respectively. Integrals of this type are called Sommerfeld integrals, and they have been widely discussed in literature since their derivation in 1920's. Numerical challenges are due to the rapid variation of the integrand as a function of b. Only the simple case of the perfectly conducting earth is straightforward. Then $N^2 \to \infty$ and the secondary field is due to a mirror dipole at $(0, 0, -h)$.

A related problem of a horizontal electric dipole is left as an exercise. According to the superposition principle, knowing the fields of vertical and electric dipoles makes it possible to determine the field of a general current system with an arbitary horizontal and vertical distribution. Even a more general case with oblique currents could be handled starting from a tilted dipole. However, in many cases it is more convenient to first specify the current distribution and then solve the fields directly without using dipoles explicitly. The next section deals with such an example.

5.3 Horizontal current sheet above a layered earth

A simple model of ionospheric currents is an infinitely long thin sheet, whose density may vary tranverse to the current flow:

$$\mathbf{J}(\mathbf{r}, \omega) = I(\omega) f(x) \delta(z + h) \mathbf{e}_y \tag{5.18}$$

where $I(\omega)$ is the Fourier amplitude of the current at frequency ω and the current flows into the y direction at height h above the earth. Here we use the conventional coordinate system in geomagnetism: the earth's surface is the xy plane and the z-axis points downwards. It is also typical to assume that x is northwards and y eastwards. The density function f is real. If there is a non-zero total current into the y direction then it is appropriate to normalise f so that $\int f(x)dx = 1$. We assume that the earth has N uniform layers.

The use of the Cartesian geometry is reasonable in regional studies, where the earth's curvature is ignorable. The assumption of an infinitely long current is a good approximation in studies of ionospheric electrojets in auroral latitudes or at the equator. These currents are east-west oriented and their lengths can be more than 1000 km. This model lacks currents along the geomagnetic field lines between the ionosphere and magnetosphere. However, if we are only interested in the field below the ionosphere this is not a restriction. Without a strict proof we mention that the true three-dimensional ionospheric current system can be replaced by an equivalent system at the ionospheric altitude, producing the same electromagnetic field below the ionosphere. As a demonstration of the equivalent theorem, the following exercise is left for the reader: show that a vertical line current arriving at the ionospheric plane produces the same magnetic field below the ionosphere as a uniformly converging radial current at the ionospheric plane.

The model current density is divergence-free, so there is no charge accumulation. This is a good assumption with true ionospheric currents: the conductivity along the field lines is very high, so excess charges are rapidly carried away as field-aligned currrents. The good conductivity parallel to the field is understandable based on the magnetic Lorentz force. A more detailed treatment of ionospheric (anisotropic) conductivities belongs to plasma physics, and is neglected here.

The assumption of the layered earth makes an analytic approach feasible. The earth's conductivity can vary very much laterally especially in the crust (the uppermost tens of kilometres), and also in the upper mantle. Deeper the conductivity mainly depends on depth only.

The calculation of the primary field is probably easiest with the vector potential. Due to the translation symmetry parallel to the current, there is no y-dependence. An exercise is to show that the electric field has only a y-component

$$E_{py} = \frac{\omega\mu_0 I(\omega)}{4}\int_{-\infty}^{\infty} dx'\ f(x')H_0^{(2)}(-k_0\sqrt{(x'-x)^2+(z+h)^2}) \qquad (5.19)$$

where $H_0^{(2)}$ is the 0th order Hankel function of the 2nd kind. The magnetic

field has two components,

$$B_{px} = \frac{i\mu_0 k_0 I(\omega)}{4} \int_{-\infty}^{\infty} dx' \; f(x') \frac{(z+h) H_1^{(2)}(-k_0 \sqrt{(x'-x)^2 + (z+h)^2})}{\sqrt{(x'-x)^2 + (z+h)^2}} \tag{5.20}$$

$$B_{pz} = \frac{i\mu_0 k_0 I(\omega)}{4} \int_{-\infty}^{\infty} dx' \; f(x') \frac{(x'-x) H_1^{(2)}(-k_0 \sqrt{(x'-x)^2 + (z+h)^2})}{\sqrt{(x'-x)^2 + (z+h)^2}} \tag{5.21}$$

where $H_1^{(2)}$ is the 1st order Hankel function of the 2nd kind. The wave number k_0 is defined by

$$\begin{aligned} k_0^2 &= \omega^2 \mu_0 \epsilon_0 + i\omega\mu_0\sigma_0 \\ 0 \leq arg(k_0) &\leq \pi/4, \; \omega > 0 \\ 3\pi/4 \leq arg(k_0) &\leq \pi, \; \omega < 0 \end{aligned} \tag{5.22}$$

It is important to understand the phase restrictions, because they must be treated correctly in the inverse Fourier transform.

As a sidenote we explain the slightly strange-looking way to write the argument of the Hankel function. If we had the harmonic time-dependence defined as $e^{+i\omega t}$ then, for example, the electric field would be

$$E_{py} = -\frac{\omega\mu_0 I(\omega)}{4} \int_{\infty}^{\infty} dx' \; f(x') H_0^{(2)}(k_0 \sqrt{(x'-x)^2 + (z+h)^2})$$

with the wave number definition

$$\begin{aligned} k_0^2 &= \omega^2 \mu_0 \epsilon_0 - i\omega\mu_0\sigma_0 \\ -\pi/4 \leq arg(k_0) &\leq 0, \; \omega > 0 \\ -\pi \leq arg(k_0) &\leq -3\pi/4, \; \omega < 0 \end{aligned}$$

In geomagnetism, $e^{+i\omega t}$ is quite commonly used.

The expressions of the primary fields are valid at all frequencies. It is easy to show that the magnetic field reduces to the Biot-Savart law at the limit of a small wave number (large wavelength), which is equivalent to studying the limit $\omega \to 0$.

Next, the secondary field in the air and the earth is to be solved. The layer structure has only a z-dependence and the primary field has only x- and z-dependence, so it is clear that the secondary field cannot depend on y. In each layer, including the air, the homogeneous wave equation of the vector potential $\mathbf{A} = A\mathbf{e}_y$ is thus

$$(\nabla^2 + k_n^2) A(x, z, \omega) = 0 \tag{5.23}$$

Separation of variables leads to the solution in each layer $n = 0, 1, ..., N$

$$E_y^n(x,z) = \int_{-\infty}^{\infty} db\ e^{ibx}(D_n(b)e^{K_n(b)z} + G_n(b)e^{-K_n(b)z}) \tag{5.24}$$

Here b must be real to have finite fields at infinity. The generalised wave number K is defined as in Eq. 5.9. The requirement of finite fields leads to the condition $G_0 = D_N = 0$. Faraday's law provides the secondary magnetic field:

$$B_x^n(x,z) = \frac{i}{\omega}\int_{-\infty}^{\infty} db\ e^{ibx}K_n(b)(D_n(b)e^{K_n(b)z} - G_n(b)e^{-K_n(b)z}) \tag{5.25}$$

$$B_z^n(x,z) = \frac{1}{\omega}\int_{-\infty}^{\infty} db\ e^{ibx}b(D_n(b)e^{K_n(b)z} + G_n(b)e^{-K_n(b)z}) \tag{5.26}$$

There are still $2N$ unknown coefficients $G_1, ..., G_N; D_0, ..., D_{N-1}$. To solve them, we apply the continuity of the horizontal fields at surfaces $z = z_0, ..., z_{N-1}$. Inside the earth at $z = z_1, ..., z_{N-1}$ we obtain

$$\begin{aligned} D_n e^{K_n z_n} + G_n e^{-K_n z_n} &= D_{n+1}e^{K_{n+1}z_{n+1}} + G_{n+1}e^{-K_{n+1}z_{n+1}} \\ \frac{K_n}{\mu_n}(D_n e^{K_n z_n} - G_n e^{-K_n z_n}) &= \frac{K_{n+1}}{\mu_{n+1}}(D_{n+1}e^{K_{n+1}z_{n+1}} - G_{n+1}e^{-K_{n+1}z_{n+1}}) \end{aligned} \tag{5.27}$$

There are $2N-2$ equations for $2N-1$ unknowns $(D_0, ...D_{N-1}; G_1, ...G_{N-1})$. So it is possible to solve $2N-2$ of them, formally as follows:

$$\begin{aligned} D_n(b) &= \alpha_n(b)G_1(b) \\ G_n(b) &= \beta_n(b)G_1(b) \end{aligned} \tag{5.28}$$

where $n = 1, ..., N$ and $\alpha_N(b) = 0, \beta_1(b) = 1$. Multipliers α_n, β_n depend on the electromagnetic parameters and thicknesses of the earth layers and on frequency.

Application of the boundary conditions at the earth's surface requires more effort. Continuity of the electric field implies

$$\begin{aligned} \frac{\omega\mu_0 I}{4}\int_{-\infty}^{\infty} dx'\ f(x')H_0^{(2)}(-k_0\sqrt{(x'-x)^2+h^2}) \quad + \quad \int_{-\infty}^{\infty} db\ e^{ibx}D_0(b) = \\ \int_{-\infty}^{\infty} db\ e^{ibx}(D_1(b) + G_1(b)) \end{aligned} \tag{5.29}$$

and continuity of B_x/μ yields

$$\begin{aligned} \frac{k_0 h I}{4}\int_{-\infty}^{\infty} dx'\ f(x')\frac{H_1^{(2)}(-k_0\sqrt{(x'-x)^2+h^2})}{\sqrt{(x'-x)^2+h^2}} \quad + \\ \frac{1}{\omega\mu_0}\int_{-\infty}^{\infty} db\ e^{ibx}K_0(b)D_0(b) = \\ \frac{1}{\omega\mu_1}\int_{-\infty}^{\infty} db\ e^{ibx}K_1(b)(D_1(b) - G_1(b)) \end{aligned} \tag{5.30}$$

Multiplication by $e^{-b'x}$ and integration with respect to x from $-\infty$ to ∞ yields, with some help from integration tables,

$$\begin{aligned} \frac{i\omega\mu_0 I e^{-K_0 h} F(b)}{4\pi K_0} + D_0(b) &= D_1(b) + G_1(b) \\ -\frac{i\omega I e^{-K_0 h} F(b)}{4\pi} + \frac{K_0}{\mu_0} D_0(b) &= \frac{K_1}{\mu_1}(D_1(b) - G_1(b)) \end{aligned} \tag{5.31}$$

where

$$F(b) = \int_{-\infty}^{\infty} dx\ e^{-ibx} f(x) \tag{5.32}$$

It is convenient to define the surface impedance:

$$Z(b) = -\frac{E_y(b,0+)}{H_x(b,0+)} = -\mu_1 \frac{E_y(b,0+)}{B_x(b,0+)} = -\frac{i\omega\mu_1}{K_1(b)} \frac{1+\alpha(b)}{1-\alpha(b)} \tag{5.33}$$

where $E_y(b,0+) = \lim_{z\to 0+} E_y(b,z)$ refers to the field just below the earth's surface. Note that $E_y(0+) = E_y(0-)$ is always true, but $B_x(0+) \neq B_x(0-)$ if $\mu_0 \neq \mu_1$. In practice the surface impedance is calculated from a recursion formula. Using $Z(b)$, the total fields just above the earth's surface ($z = 0-$) are

$$E_y(x,\omega) = -\frac{i\omega\mu_0 I(\omega)}{2\pi} \int_{-\infty}^{\infty} db\ e^{ibx}\ \frac{Z(b)F(b)e^{-K_0 h}}{i\omega\mu_0 - K_0 Z(b)} \tag{5.34}$$

$$B_x(x,\omega) = \frac{i\omega\mu_0^2 I(\omega)}{2\pi} \int_{-\infty}^{\infty} db\ e^{ibx}\ \frac{F(b)e^{-K_0 h}}{i\omega\mu_0 - K_0 Z(b)} \tag{5.35}$$

$$B_z(x,\omega) = -\frac{i\mu_0 I(\omega)}{2\pi} \int_{-\infty}^{\infty} db\ e^{ibx}\ \frac{bZ(b)F(b)e^{-K_0 h}}{i\omega\mu_0 - K_0 Z(b)} \tag{5.36}$$

An exercise is to show that the surface impedance can be calculated by the following recursion formula:

$$\begin{aligned} Z_1 &= -\frac{i\omega\mu_N}{K_N} \\ Z_2 &= -\frac{i\omega\mu_{N-1}}{K_{N-1}} \coth(K_{N-1}h_{N-1} - \coth^{-1}(\frac{K_{N-1}Z_1}{\omega\mu_{N-1}})) \\ &\ldots \\ Z_N &= -\frac{i\omega\mu_1}{K_1} \coth(K_1 h_1 - \coth^{-1}(\frac{K_1 Z_{N-1}}{\omega\mu_1})) \end{aligned} \tag{5.37}$$

It is occasionally more illustrative to write the primary and secondary contributions separately. Then the expressions of the fields in the air ($z < 0$) are

$$\begin{aligned} E_y(x,z,\omega) = \frac{i\omega\mu_0 I(\omega)}{4\pi} \int_{-\infty}^{\infty} db\ \frac{F(b)e^{ibx}}{K_0} (e^{-K_0|z+h|} \\ -\frac{i\omega\mu_0 + K_0 Z(b)}{i\omega\mu_0 - K_0 Z(b)} e^{K_0(z-h)}) \end{aligned} \tag{5.38}$$

$$B_x(x,z,\omega) = \frac{\mu_0 I(\omega)}{4\pi}\int_{-\infty}^{\infty} db\ F(b)e^{ibx}(sgn(z+h)e^{-K_0|z+h|} + \frac{i\omega\mu_0 + K_0 Z(b)}{i\omega\mu_0 - K_0 Z(b)}e^{K_0(z-h)}) \tag{5.39}$$

$$B_z(x,z,\omega) = \frac{i\omega\mu_0 I(\omega)}{4\pi}\int_{-\infty}^{\infty} db\ \frac{bF(b)e^{ibx}}{K_0}(e^{-K_0|z+h|} - \frac{i\omega\mu_0 + K_0 Z(b)}{i\omega\mu_0 - K_0 Z(b)}e^{K_0(z-h)}) \tag{5.40}$$

The first terms in the integrands correspond to the primary field, and the second parts to the secondary field, respectively (cf. the dipole field).

These integrals cannot generally be evaluated in a closed form. Due to rapidly oscillating integrands, numerical problems are similar to those with Sommerfeld integrals. However, in low-frequency problems there are convenient approximation techniques based on the method of images.

5.3.1 Divergence-free elementary current system

A handy way to express a general horizontal current distribution is to use elementary current systems[1]. We concentrate here in the geomagnetic problem where the fields below the ionosphere are of interest. As mentioned in Sect. 5.3, only the divergence-free part of the current system produces a field below the ionosphere. For simplicity, we will assume a quasi-dc case, but the following could be generalised to an arbitary time-dependence too. Further, we study only a planar geometry, which is an acceptable assumption in local studies.

The surface current density of a divergence-free elementary system with amplitude I at height h in cylindrical coordinates ($r = \sqrt{x^2+y^2}$) is

$$\mathbf{J}(r) = \frac{I}{2\pi r}\ \mathbf{e}_\phi \tag{5.41}$$

A realistic ionospheric current system can be constructed with a set a suitably placed elements whose amplitudes are fitted to yield the measured ground magnetic field. Pulkkinen et al. (2003)[2] provide a detailed validation.

[1] Amm, O. and A. Viljanen, Ionospheric disturbance magnetic field continuation from the ground to the ionosphere using spherical elementary current systems. Earth, Planets and Space, 51, 431-440, 1999.

[2] Pulkkinen, A., O. Amm, A. Viljanen and BEAR Working Group, Ionospheric equivalent current distributions determined with the method of spherical elementary current systems, J. Geophys. Res., 108(A2), 1053, doi:10.1029/2001JA005085, 2003.

An exercise is to derive the primary electric field at the earth's surface due to a single elementary system:

$$\mathbf{E} = \frac{i\omega\mu_0 I}{4\pi} \frac{\sqrt{r^2+h^2}-h}{r} \mathbf{e}_\phi \tag{5.42}$$

where the z axis points vertically downwards and the earth's surface is the xy plane and a harmonic time-dependence ($e^{-i\omega t}$) is assumed. The primary magnetic field is

$$\mathbf{B} = \frac{\mu_0 I}{4\pi r} \left((1 - \frac{h}{\sqrt{r^2+h^2}}) \mathbf{e}_r + \frac{r}{\sqrt{r^2+h^2}} \mathbf{e}_z \right) \tag{5.43}$$

The secondary fields due to induced currents in the earth could be solved in the similar way as presented in Sect. 5.3, although it would be more laborious. Instead, in geomagnetic problems we can apply the method of images with a good accuracy (Sect. 5.4.2).

5.4 Method of images

The method of images is based on the uniqueness of the solutions of the Maxwell equations. In many applications, we are only interested in the electromagnetic in a restricted domain. The rest of the space can be replaced by a charge and current distribution providing that the Maxwell equations are fulfilled in the domain considered. Furthermore, the correct boundary conditions must be satisfied at the surface of the area of interest. The advantage of the method is that sometimes the image source has a sufficiently simple form to allow for a convenient calculation of the field. The basic example is a point charge q above an infinite grounded conductor plane. The task is to determine the electric field above the plane. Noting that the appropriate boundary condition is a zero potential at the plane, the conductor can be replaced by a mirror charge $-q$. The field above the plane is just the sum of the fields of the two point charges. A more general example is a point charge close to a planar boundary between two insulators with different permittivities. Now the solution requires two image charges (see the lecture notes of electrodynamics).

Here we will consider two techniques utilising the method of images. The first is the exact image theory (EIT) developed at the Helsinki University of Technology (HUT). It is actually an alternative way to derive the exact solution of the half-space problem. The expressions obtained can be interpreted in terms of image sources. Another technique is an older approximation method starting from the exact traditional solution of the half-space problem. It must be remembered that image sources are not true physical objects. However, the concreteness of the image concept is useful for physical understanding of some basic features of fields.

5.4.1 Exact image theory

The exact image theory was developed at HUT in 1980's, and since then it has been widely used in several applications. It is also a nice example of how it is still possible to find new analytical approaches using the Maxwell equations.

We start from the expression of the Hertz vector $\mathbf{\Pi} = \Pi \mathbf{e}_z$ due to a vertical dipole at height h above a uniform earth (Eq. 5.17):

$$\Pi = \frac{IL}{4\pi(\sigma_0 - i\omega\epsilon_0)} \int_0^\infty db \; \frac{b}{K_0}(e^{-K_0|z-h|} + \frac{N^2K_0 - K_1}{N^2K_0 + K_1} e^{-K_0(z+h)}) J_0(b\rho) \tag{5.44}$$

where

$$N^2 = \frac{\sigma_1 - i\omega\epsilon_1}{\sigma_0 - i\omega\epsilon_0} \tag{5.45}$$

The expression of the Hertz vector is valid in the air ($z > 0$; note the different direction of the z-axis compared to the previous section). In the following we drop off the subscript 0 for brevity, so now $K_1 = \sqrt{b^2 - k_1^2} = \sqrt{K^2 + k^2 - k_1^2}$.

EIT starts with manipulating the reflection coefficient

$$R(K) = \frac{N^2K - K_1}{N^2K + K_1} = \frac{N^2K - \sqrt{K^2 + k^2 - k_1^2}}{N^2K + \sqrt{K^2 + k^2 - k_1^2}} \tag{5.46}$$

The basic idea is to express $R(K)$ as a Laplace transform

$$R(K) = \int_0^{\infty e^{i\alpha}} db \; f(b) e^{-bK} \tag{5.47}$$

where the integration path in the complex b plane is a straight line from the origin with $arg(b) = \alpha$. To get a converging result, α must be suitably selected. So far, $f(b)$ is not explicitly specified.

Now the Hertz vector can be written as

$$\begin{aligned}\Pi = \frac{IL}{4\pi(\sigma - i\omega\epsilon)} (& \int_0^\infty db \; \frac{b}{K}(e^{-K|z-h|} J_0(b\rho) + \\ & \int_0^{\infty e^{i\alpha}} f(b) \int_0^\infty db \; \frac{b}{K} e^{-K(z+h+b)} J_0(b\rho))\end{aligned} \tag{5.48}$$

So it is possible to interpret that the secondary (reflected) field is due to image dipoles $ILf(b)\mathbf{e}_z$ at complex points $(0, 0, -h - b)$ in a uniform material with electromagnetic parameters (μ, ϵ, σ). By changing the integration

variable ($z' = -b - h$) we can write the secondary Hertz vector as

$$\Pi_{sec} = -\frac{IL}{4\pi(\sigma - i\omega\epsilon)} \int_{-h}^{-h-\infty e^{i\alpha}} dz' \; f(-z'-h) \int_0^\infty db \; \frac{b}{K} e^{-K(z-z')} J_0(b\rho)) \tag{5.49}$$

The integral with respect to b is known from Sect. 5.2, so we obtain for the total Hertz vector

$$\Pi = -\frac{IL}{4\pi(\sigma - i\omega\epsilon)} (\frac{e^{ikr}}{r} - \int_{-h}^{-h-\infty e^{i\alpha}} dz' \; f(-z'-h) \frac{e^{ikr'}}{r'}) \tag{5.50}$$

Here $r = \sqrt{\rho^2 + (z-h)^2}$ is the real distance from the primary dipole to the observation point, and $r' = \sqrt{\rho^2 + (z-z')^2}$ is the complex distance from the image source to the observer.

The problem of selecting the correct integration path is complicated. We will restrict the investigation to two simple examples. The first one is a perfectly conducting earth corresponding to $R(K) = 1$. This leads to selecting $\alpha = 0$ and $f(b) = \delta(b+) = \lim_{a \to 0+} \delta(b-a)$ in Eq. 5.47. The image source is thus $IL\delta(x)\delta(y)\delta(z+h)$, which is the expected result.

In the second example we assume that the permittivity and conductivity of the earth are equal to the values in the air, but that the permeability is $\mu_1 = \mu_r \mu_0$ with $\mu_r \neq 1$. Now $N^2 = 1$ and

$$R(K) = \frac{K - \sqrt{K^2 + (1-\mu_r)k^2}}{K + \sqrt{K^2 + (1-\mu_r)k^2}} \tag{5.51}$$

Using a table of Laplace transforms (Abramowitz & Stegun, 1972, 29.3.58) we get

$$R(K) = -\int_0^{\infty e^{i\alpha}} db \; \frac{2e^{-Kb}}{b} J_2(ikb\sqrt{\mu_r - 1}) \tag{5.52}$$

so

$$f(b) = -\frac{2}{b} J_2(ikb\sqrt{\mu_r - 1}) \tag{5.53}$$

The argument of the Bessel function J_2 must be real to have a converging integral. So we must have $arg(b) + arg(ik\sqrt{\mu_r - 1}) = 0$, i.e. $\alpha = -arg(ik\sqrt{\mu_r - 1})$. The secondary Hertz vector is

$$\Pi_{sec} = -\frac{IL}{2\pi(\sigma - i\omega\epsilon)} \int_{-h}^{-h-\infty e^{i\alpha}} dz' \; \frac{J_2(-ik\sqrt{\mu_r - 1}(z'+h))}{z'+h} \; \frac{e^{ikr'}}{r'} \tag{5.54}$$

The change of variable

$$z' + h = -\frac{p}{ik\sqrt{\mu_r - 1}}$$

yields

$$\Pi_{sec} = -\frac{IL}{2\pi(\sigma - i\omega\epsilon)} \int_0^\infty dp \; \frac{J_2(p)}{p} \; \frac{e^{iks(p)}}{s(p)} \tag{5.55}$$

where

$$s(p) = \sqrt{\rho^2 + (z + h + \frac{p}{ik\sqrt{\mu_r - 1}})^2} \tag{5.56}$$

The Hertz vector may still look cumbersome. However, the term $J_2(p)/p$ in the integral is well-behaving, since it attenuates very quickly as a function of p.

5.4.2 Wait's image approximation

The image method for geophysical applications was first presented by Wait[3], and later by several other authors. Here we follow quite closely the presentation by Thomson and Weaver[4]. Although we derive the image depth only for a specific type of ionospheric currents of Sect. 5.3, the same result holds for any horizontal system such as the one discussed in Sect. 5.3.1. We could also use EIT here, but the following derivation is easier for this specific purpose.

In geomagnetic induction problems, time-variations of the field are so slow that the displacement current in the earth is ignorable ($\omega\epsilon \ll \sigma$). Then as the first approximation, the earth below an ionospheric current system could be replaced by a perfect conductor at some depth d below the surface. The larger the real conductivity of the earth, the closer to the surface the perfect conductor would be placed. Such a model is qualitatively good giving the correct behaviour of the fields: the horizontal magnetic field tends to increase, whereas the vertical component decreases compared to the situation in an empty space. The horizontal electric field decreases and the vertical field increases.

A more accurate approximation starts from the exact formula of the electric field due to a sheet currrent above a layered earth (Eq. 5.38):

$$\begin{aligned} E_y(x,z,\omega) = \frac{i\omega\mu_0 I(\omega)}{4\pi} \int_{-\infty}^{\infty} db\, \frac{F(b)e^{ibx}}{K_0} (e^{-K_0|z+h|} \\ - \frac{i\omega\mu_0 + K_0 Z(b)}{i\omega\mu_0 - K_0 Z(b)} e^{K_0(z-h)}) \end{aligned} \tag{5.57}$$

which is valid in the air (here $z < 0$). Without losing generality, we can study a line current for which $F(b) = 1$. Further, we assume a uniform earth with $\mu_1 = \mu_0, Z(b) = -i\omega\mu_0/K_1$. Now the electric field is (exactly)

$$E_y(x,z,\omega) = \frac{i\omega\mu_0 I(\omega)}{4\pi} \int_{-\infty}^{\infty} db\, \frac{e^{ibx}}{K_0} (e^{-K_0|z+h|} + \frac{K_0 - K_1}{K_0 + K_1} e^{K_0(z-h)}) \tag{5.58}$$

[3]Wait, J.R., Image theory of a quasi-static magnetic dipole over a dissipative ground. Electr. Lett., 5, 281–282, 1969.

[4]Thomson, D.J. and J.T. Weaver, The Complex Image Approximation for Induction in a Multilayered Earth. J. Geophys. Res., 80, 123-129, 1975.

Next, we neglect the displacement current, and approximate

$$\begin{aligned} K_0 &\approx \sqrt{b^2 - k_0^2} \\ K_1 &\approx \sqrt{b^2 - i\omega\mu_0\sigma_1} = u(b) = \sqrt{b^2 + g^2} \end{aligned}$$

Note that the parameter g is proportional to the skin depth $\sqrt{2/(\omega\mu_0\sigma)}$ in a uniform medium. Now the electric field is

$$E_y(x,\omega) \approx \frac{i\omega\mu_0 I(\omega)}{2\pi} \int_0^\infty db\ \frac{\cos bx}{b}(e^{-b|z+h|} + \frac{b-u(b)}{b+u(b)} e^{b(z-h)}) \tag{5.59}$$

The aim is to write the latter term in the brackets in a purely exponential form. For that, consider the function

$$f(b) = \frac{b-u(b)}{b+u(b)} e^{\alpha b} \tag{5.60}$$

where α is a parameter to be selected appropriately. The Taylor expansion at the origin yields

$$f(b) = -1 + (\frac{2}{g} - \alpha)b - \frac{(2-\alpha g)^2}{2g^2} b^2 + (\frac{1}{g^3} - \frac{2\alpha}{g^2} + \frac{\alpha^2}{g} - \frac{\alpha^3}{6})b^3 + ... \tag{5.61}$$

If we choose $\alpha = 2/g$ we get

$$f(b) = -1 + \frac{b^3}{3g^3} + ... \tag{5.62}$$

The lower the frequency the smaller are b-dependent terms compared to unity.

Taking only the first term of the series of $f(b)$ the electric field is

$$E_y(x,z,\omega) \approx \frac{i\omega\mu_0 I(\omega)}{2\pi} \int_0^\infty db\ \frac{\cos bx}{b}(e^{-b|z+h|} + e^{b(z-(h+2/g))}) \tag{5.63}$$

The great advantage is that the integral can be evaluated analytically (Gradshteyn & Ryzhik, 1980, 3.951.3):

$$E_y(x,z,\omega) \approx \frac{i\omega\mu_0 I(\omega)}{2\pi} \ln \frac{R_1}{R_0} \tag{5.64}$$

where R_0 and R_1 are the distances from the primary line current and image current to the observation point:

$$\begin{aligned} R_0 &= \sqrt{x^2 + (z+h)^2} \\ R_1 &= \sqrt{x^2 + (z-h-2/g)^2} \end{aligned} \tag{5.65}$$

It is possible to interpret that the image current flows at a complex depth $h + 2/g = h + (1+i)\delta$, where $\delta = \sqrt{2/(\omega\mu_0\sigma)}$ is the skin depth. It is good to remember that the image source is not real, but just a mathematical concept. Furthermore, the expression of the field is valid only above the earth's surface ($z < 0$). This derivation assumed a uniform earth. The complex image depth for a general layered structure is

$$p(\omega) = -\frac{Z(\omega)}{i\omega\mu_0} \tag{5.66}$$

where $Z(\omega)$ is the surface impedance of the plane wave. The proof of this result is left as an exercise.

5.4.3 Electrostatic image of an insulating sphere

We finish the expedition in image methods with an electrostatic example. Consider a uniform neutral sphere of permittivity $\epsilon_r\epsilon_0$ ja radius a. A point charge Q is placed outside of the sphere at distance b from its centre (at z axis). The conventional solution method is the expansion of the potential in spherical harmonics. It follows that outside the sphere

$$\varphi(\mathbf{r}) = \frac{Q}{4\pi\epsilon_0|\mathbf{r} - b\mathbf{e}_z|} - \frac{Q}{\epsilon_0}\sum_{n=1}^{\infty}\frac{(\epsilon_r - 1)n}{(\epsilon_r + 1)n + 1}\frac{a^{2n+1}}{b^{n+1}}\frac{P_n(\cos\theta)}{4\pi r^{n+1}} \tag{5.67}$$

The latter term is the "reflected" or "scattered" potential φ_r due to the sphere. In the image method, a charge distribution in the region $r < a$ causing the same reflected term at $r > a$ is looked for. This problem was solved independently by several authors in the end of 1900's. However, it has recently turned out that the solution was already found for more than 100 years earlier![5]

There are many possible approaches to derive the image charge. We follow the one given by Olyslager and Lindell illustrating the operator calculus invented by Heaviside in the end of 1800's. First we note that

$$\partial_z^n\frac{1}{r} = (-1)^n n!\frac{P_n(\cos\theta)}{r^{n+1}} \tag{5.68}$$

Consequently, the reflected potential is

$$\varphi_r(\mathbf{r}) = -\frac{\epsilon_r - 1}{\epsilon_r + 1}\frac{Qa}{\epsilon_0 b}\sum_{n=1}^{\infty}\frac{(-c\partial_z)^n}{(n-1)!(n+\alpha)}\frac{1}{4\pi r} \tag{5.69}$$

[5] Olyslager, F. and I. Lindell, the Radio Science Bulletin No. 305, June 2003, p. 31-32. Available on WWW: http://www.ursi.org/RSBissues/RSBjune03.pdf

where $c = a^2/b$ and $\alpha = 1/(\epsilon_r + 1)$. The image charge density ρ_r is obtained from the Poisson equation as

$$\rho_r(\mathbf{r}) = -\epsilon_0 \nabla^2 \varphi_r(\mathbf{r}) \tag{5.70}$$

The vacuum permittivity must be used here, since the whole sphere is now replaced by a charge distribution. Using the basic result

$$\nabla^2 \frac{1}{4\pi r} = -\delta(\mathbf{r}) = -\delta(z)\delta(\rho) \tag{5.71}$$

we can write the image charge density as

$$\rho_r(\mathbf{r}) = -\frac{\epsilon_r - 1}{\epsilon_r + 1}\frac{Qa}{b}\sum_{n=1}^{\infty}\frac{(-c\partial_z)^n}{(n-1)!(n+\alpha)}\delta(z)\delta(\rho) \tag{5.72}$$

This can be interpreted as a multipole expansion of the charge density. Especially, there is no monopole term (neutral sphere), and all multipoles are located at the z axis (due to $\delta(\rho)$).

To proceed, we note that

$$\rho_r(\mathbf{r}) = \frac{\partial}{\partial z}\frac{\epsilon_r - 1}{\epsilon_r + 1}\frac{Qa}{b}\sum_{n=0}^{\infty}\frac{c^{n+1}(-\partial_z)^n}{n!(n+\alpha+1)}\delta(z)\delta(\rho) = \partial_z p_r(z)\delta(\rho) \tag{5.73}$$

where $p_r(z)$ is an abbreviation corresponding to the dipole moment density. Multiplying p_r by c^α and differentiating with respect to c yields

$$\partial_c[c^\alpha p_r(z)] = \frac{\epsilon_r - 1}{\epsilon_r + 1}\frac{Qa}{b}\sum_{n=0}^{\infty}\frac{c^{n+\alpha}(-\partial_z)^n}{n!}\delta(z) \tag{5.74}$$

In the operator calculus, operators are formally handled as normal numbers, so

$$\partial_c[c^\alpha p_r(z)] = \frac{\epsilon_r - 1}{\epsilon_r + 1}\frac{Qa}{b}c^\alpha e^{-c\partial_z}\delta(z) = \frac{\epsilon_r - 1}{\epsilon_r + 1}\frac{Qa}{b}z^\alpha\delta(z-c) \tag{5.75}$$

where the proof of the last step is left as an exercise. Now we have a differential equation for p_r. Requiring that p_r vanishes for $z > a$, the solution is

$$p_r(z) = \frac{\epsilon_r - 1}{\epsilon_r + 1}\frac{Qa}{b}(z/c)^\alpha\theta(c-z)\theta(z) \tag{5.76}$$

where θ is the step function. Finally, the image charge density is

$$\rho_r(\mathbf{r}) = \frac{\epsilon_r - 1}{(\epsilon_r + 1)^2}\frac{Qa}{b}(z/c)^{-\epsilon_r/(\epsilon_r+1)}\theta(c-z)\theta(z) - \frac{\epsilon_r - 1}{\epsilon_r + 1}\frac{Qa}{b}\delta(c-z) \tag{5.77}$$

As a simple check, the familiar result of a conducting sphere follows from setting $\epsilon_r = \infty$, when the image is just a point charge $-Qa/b$ at $z = a^2/b$. In the general case, there is an additional line charge distribution along the z axis from the origin to $z = a^2/b$.

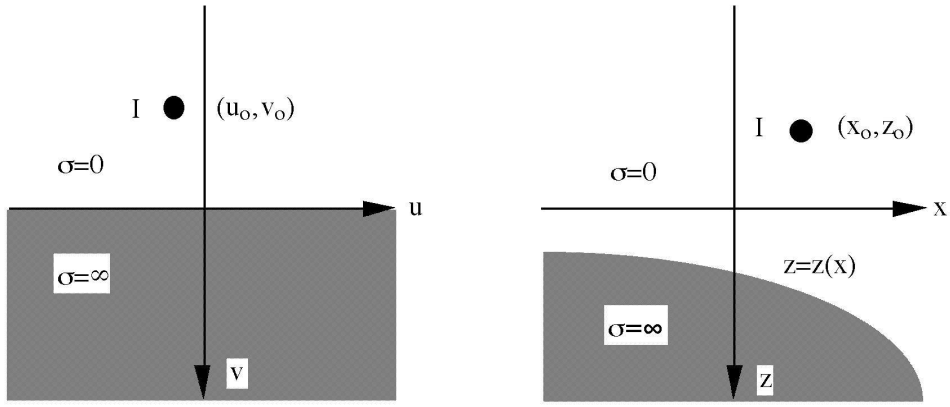

Figure 5.1: Coordinate system used in conformal mapping. The vertical axis is positive downwards as usual in geomagnetic applications. The shaded region is a perfect conductor.

5.4.4 Conformal mapping

So far we have considered one-dimensional structures in which the electromagnetic material parameters vary only in one direction. More general situations typically require a numerical solution, for example by the methods of finite differences, finite elements or integral equations. Despite the rapid growth of computer power, three-dimensional problems are still time-consuming.

An elegant way to study specific two-dimensional structures is conformal mapping. The basic idea is to first investigate a one-dimensional model and then with an appropriate coordinate transformation to go to a more complicated situation. A concrete example is perhaps the best way to illustrate the technique[6].

Use a Cartesian uyv coordinate system (Fig. 5.1) and consider a line current I flowing parallel to the y axis at (u_0, v_0). The upper half space $(v < 0)$ containing the line current is non-conducting and the lower part is a perfect conductor. In the region $v < 0$ the vector potential has only the y component

$$A(u,v) = -\frac{\mu_0 I}{4\pi} \ln \frac{(u-u_0)^2 + (v-v_0)^2}{(u-u_0)^2 + (v+v_0)^2} \tag{5.78}$$

neglecting the displacement current. The (slow) time dependence of I may be arbitrary.

Conformal mapping is a coordinate transformation $u = u(x,z), v =$

[6] Janhunen, P. and A. Viljanen, Application of conformal mapping to 2-D conductivity structures with non-uniform primary sources. Geophys. J. Int., 105, 185-190, 1991.

$v(x,z)$, where the real functions u and v satisfy the Cauchy-Riemann conditions

$$\frac{\partial u}{\partial x} = \frac{\partial v}{\partial z}\,,\ \frac{\partial u}{\partial z} = -\frac{\partial v}{\partial x} \tag{5.79}$$

Thus the complex function $f(w) = f(x+iz) = u(x,z) + iv(x,z)$ is analytic.

The procedure for a line current is as follows:

1. Choose an analytic function $f(w) = f(x+iz) = u(x,z) + iv(x,z)$.

2. Determine $z = z(x)$ from the equation $v(x, z(x)) = 0$ and check that it is physically reasonable, i.e. $z(x)$ is finite at infinity.

3. Choose the location (x_0, z_0) of the line current and calculate $(u_0, v_0) = (u(x_0, z_0), v(x_0, z_0))$ checking that $v_0 < 0$.

4. Calculate $A'(x,z) = A(u(x,z), v(x,z))$ where A is given by Eq. 5.78.

5. Calculate the magnetic and electric fields from

$$\begin{aligned} B'_x(x,z) &= -\frac{\partial A'(x,z)}{\partial z} \\ B'_z(x,z) &= \frac{\partial A'(x,z)}{\partial x} \\ E'_y(x,z) = -\frac{\partial A'(x,z)}{\partial t} &= i\omega A'(x,z) \end{aligned} \tag{5.80}$$

The explicit formula of the current density into the y-direction becomes

$$J'(x,z) = ((\frac{\partial u(x,z)}{\partial x})^2 + (\frac{\partial u(x,z)}{\partial z})^2)\ J(u(x,z), v(x,z)) \tag{5.81}$$

The magnetic field can also be written as

$$B_x(w) - iB_z(w) = \frac{i\mu_0 I}{2\pi}(\frac{1}{f(w) - f(w_0)} - \frac{1}{f(w) - f^*(w_0)})\frac{df(w)}{dw} \tag{5.82}$$

where $w = x + iz$. The main point in conformal mapping is that the vector potential satisfies the Helmholtz equation also in the xyz frame when A and J are redefined as above.

6. The curves A = constant are parallel to magnetic field lines because $\mathbf{B} \cdot \nabla A = 0$. The number of contour lines of A is proportional to the magnetic flux through a given surface. Thus, the field lines of $\mathbf{B}$ are the same as contour lines of A.

This procedure is easy to code with a symbolically calculating computer program. To verify the acceptability of f, the field line representation is convenient. Possible singularities of f and zeros of f' should also be checked. It is possible that the equation $v(x, z(x)) = 0$ does not have a single valued solution but it is not a problem in practice as seen in the example below.

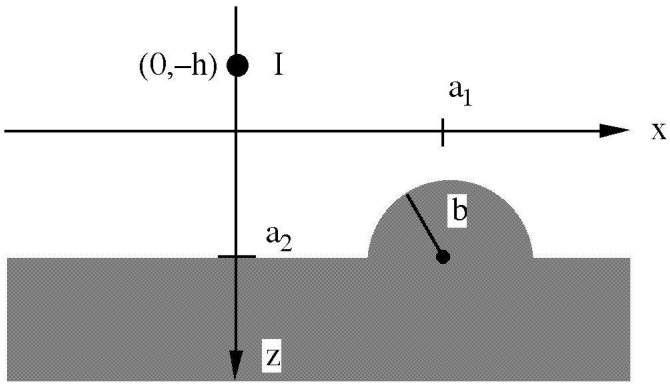

Figure 5.2: Line current and a semi-circular conductivity anomaly.

Consider a line current flowing along the line $w_0 = (x_0, z_0) = (0, -h)$ in the xyz frame. Let

$$f(w) = \frac{w-a}{b} + \frac{b}{w-a} + c \tag{5.83}$$

which gives semi-circular anomalies if $Im(c) = 0$ (Fig. 5.2), and their smoothed modifications if $Im(c) \neq 0$. Choose $a = a_1 + ia_2$ (a_1 real, $a_2 > 0$), $b > 0$ and $c = 0$ which allows us to write the results in a closed form. The imaginary part of f is

$$v(x,z) = \frac{z-a_2}{b} - \frac{b(z-a_2)}{(x-a_1)^2 + (z-a_2)^2} \tag{5.84}$$

The zeros can be solved exactly and the curve $z = z(x)$ can be defined as

$$\begin{aligned} z = a_2\,,\ x \leq a_1 - b \text{ or } x \geq a_1 + b \\ (x-a_1)^2 + (z-a_2)^2 = b^2\,,\ a_1 - b \leq x \leq a_1 + b\,,\ z \leq a_2 \end{aligned} \tag{5.85}$$

It is evident from the field line presentation (Fig. 5.3) that the perfect conductor can be replaced by a few concentrated image currents. In this example, they are line currents as seen from the expansion in partial fractions:

$$B_x(w) - iB_z(w) = \frac{i\mu_0 I}{2\pi} \sum_n \frac{c_n}{w - w_n} \tag{5.86}$$

An exercise is to show that the sum of the amplitudes of the image currents is $-I$ and that $\sum c_n Re(w_n) = 0$.

If the primary field is a plane wave then $A(v) = -B_0 v$ where B_0 is constant. The field in the xyz coordinates is

$$B_x(x,z) = B_0 \frac{\partial v(x,z)}{\partial z}$$

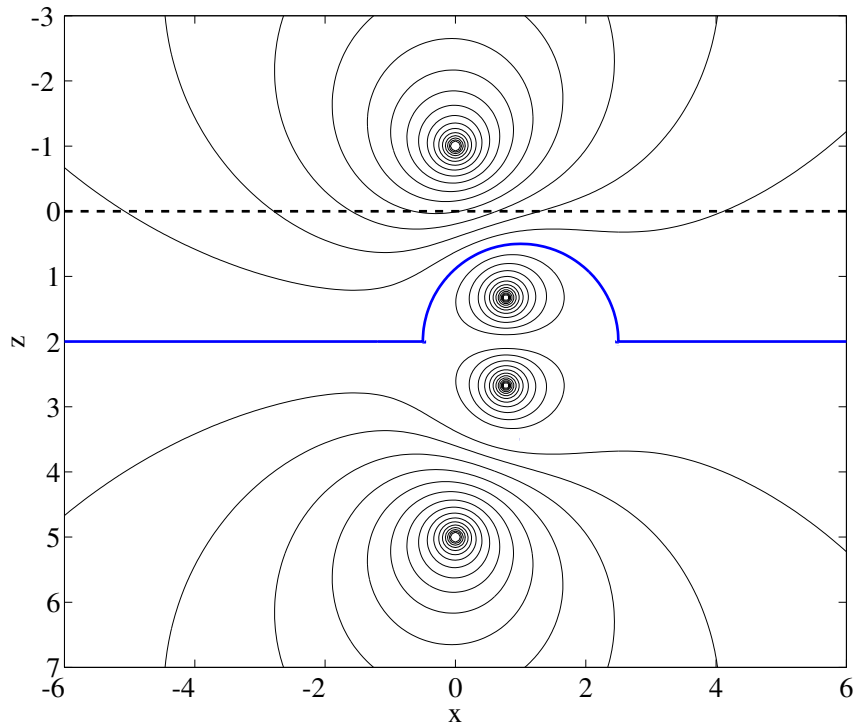

Figure 5.3: A line current at $x = 0, z = -1$ is located close to a semi-circular conductivity anomaly centred at $x = 1, z = 2$ and having a radius 1.5. The blue curve is the isoline $v(x, z) = 0$, which represents the surface of the perfect conductor. The dashed line is the earth's surface. An exercise is to add the direction of the field in the field lines.

$$\begin{aligned} B_z(x,z) &= -B_0 \frac{\partial v(x,z)}{\partial x} \\ E_y(x,z) &= i\omega B_0 v(x,z) \end{aligned} \tag{5.87}$$

The magnetic field lines are determined by the equation $v(x, z) = \text{constant}$. The plane wave field can be expressed as

$$B_x(w) - iB_z(w) = B_0 \frac{df(w)}{dw} \tag{5.88}$$

It is an exercise to study the plane wave using the same anomaly as with the line current in the example above.

5.5 Geomagnetic induction

There are complicated electric currents systems in the Earth's magnetosphere and ionosphere, which are primarily maintained by the interaction of

the solar wind and the geomagnetic field. Irregular variations in the solar wind manifest themselves as temporal changes of the near space currents and the magnetic field. The largest magnetic storms cause disturbances whose amplitudes at the earth's surface are some thousands of nT at maximum. Typical periods vary from seconds to hours.

Due to the time-dependence of the magnetic field, there is always an associated electric field too. This geoelectric field causes currents in all conductors including the earth. It follows that the varying magnetic and electric fields measured at the surface have two sources: primary space currents and secondary induced currents in the earth (telluric currents). So a measurement of these fields can provide information both of the near-space and the ground.

Mathematically, this is a half-space problem already considered in this chapter. Consequently, we could apply the full machinery with realistic models of ionospheric currents and of a layered earth. However, that would be beyond the scope of this course, so we just present the basis of the magnetotelluric sounding method. It allows for a simple analytic treatment and reveals several generally valid features of the induced fields. As a Finnish speciality, we present modelling of geomagnetically induced currents in power systems and pipelines.

Geomagnetic recordings are a routine method to study ionospheric currents. Combined with other measurements such as observations of the ionospheric electric fields with radars, they provide information of the ionospheric electrodynamics. On the other hand, magnetic recordings are useful also in investigations of the earth's conductivity structure. A combination with measurements of the geoelectric field provides even more power to such studies. In Finland, ionospheric studies with ground-based methods have been widely performed at FMI and the University of Oulu. The MIRACLE[7] network headed by FMI is one of the best instrument systems for mesoscale ionospheric studies. Solid earth studies with natural EM fields have been performed widely by the University of Oulu.

5.5.1 Magnetotellurics

Magnetotellurics is a method to sound the earth's structure by electromagnetic measurements at the earth's surface. The fields measured are the magnetic field $\mathbf{B} = (B_x, B_y, B_z)$ and the horizontal electric field $\mathbf{E}_{hor} = (E_x, E_y)$ (exercise: why the vertical electric field is not used?). The magnetic field is recorded by a fluxgate magnetometer, for example (exercise: study its principle in literature). The electric field is measured by electrodes buried in the

[7] http://www.ava.fmi.fi/MIRACLE/

earth, so the voltage between the electrode plates is the primary quantity. Exercise: what practical difficulties there are especially with the recordings of the electric field?

The magnetotelluric method requires that there is a time-varying field. It can be the natural field due to geomagnetic variations, or the primary field can be produced by a controlled source. We present here the classical model by Cagniard[8] and Tikhonov[9] with a plane wave source and a layered earth.

The simplest case of a uniform earth is familiar from the electrodynamics course: it is just the reflection of a vertically propagating plane wave at the surface of an ohmic conductor. We assume in the following that the permeability has its vacuum value everywhere. It is an exercise for the reader to repeat the exact calculus to show that at the earth's surface (xy plane) the horizontal electric and magnetic fields are related by

$$E(\omega) = -\frac{\omega B(\omega)}{\sqrt{\omega^2\mu_0\epsilon + i\omega\mu_0\sigma}} = \frac{ig(\omega)}{\sqrt{\omega^2\mu_0\epsilon + i\omega\mu_0\sigma}} \tag{5.89}$$

where $E = E_y, g = dB_x/dt$. At low frequencies, a good approximation is

$$E(\omega) = \sqrt{\frac{i}{\omega\mu_0\sigma}}\, g(\omega) \tag{5.90}$$

The total magnetic field at the earth's surface is related to the primary field B_0 as follows:

$$B(\omega) = \frac{2k}{k_0 + k} B_0(\omega) \tag{5.91}$$

and the corresponding equation for the electric field is

$$E(\omega) = \frac{2k_0}{k_0 + k} E_0(\omega) \tag{5.92}$$

Consequently, at geomagnetic frequencies induction in the earth practically doubles the plane wave magnetic field, but nearly cancels the horizontal electric field. In other words, the earth is quite close to a perfect conductor in geomagnetic induction problems. This is qualitatively true also for more complicated primary sources.

Returning back to the relation between the fields, we note that the surface impedance is

$$Z(\omega) = -\frac{E_y(z=0)}{H_x(z=0)} = -\frac{\mu_0 E_y(z=0)}{B_x(z=0)} = \frac{\omega\mu_0}{k} = \frac{E_x(z=0)}{H_y(z=0)} \tag{5.93}$$

[8] Cagniard, L., Basic theory of the magneto-telluric method of geophysical prospecting. Geophysics, 18, 605-635, 1953.

[9] Tikhonov, A.N., Determination of the electrical characteristics of the deep strata of the earth's crust (Russian). Dok. Akad. Nauk, USSR, 73, 295-297, 1950.

So the relation of the electric field to the magnetic field depends only on frequency and on the electromagnetic parameters of the earth. The same holds for a layered structure.

Measurement of the electromagnetic field is thus a way to investigate the earth's conductivity, but even in the ideal case of a plane wave and a layered earth, the inversion problem is difficult. In principle, it is possible to infer uniquely the conductivity if it is only dependent on depth[10]. However, the result is very sensitive to small errors in data. Other difficulties come from the fact that the earth's structure is not one-dimensional. Furthermore, the assumption of a plane wave source is seldom strictly valid in regions close to localised ionospheric currents (especially the auroral zone and the equatorial region). There is still a need for developing interpretation methods of magnetotelluric measurements.

The analysis of magnetotelluric data is typically performed in the frequency domain. However, the time domain demonstrates some general physical facts more clearly. In the following, we still deal with a uniform earth. To get into the time domain we must perform the inverse Fourier transform

$$E(t) = \frac{1}{\sqrt{2\pi}} \int_{-\infty}^{\infty} d\omega \; e^{-i\omega t} E(\omega) = -\frac{1}{\sqrt{2\pi}} \int_{-\infty}^{\infty} d\omega \; e^{-i\omega t} \; \frac{\omega B(\omega)}{k(\omega)} \tag{5.94}$$

Denoting $g(t) = dB(t)/dt$ we have $g(\omega) = -i\omega B(\omega)$. With the convolution theorem we obtain

$$E(t) = \frac{1}{\sqrt{2\pi}} \int_{-\infty}^{\infty} du \; g(t-u) F(u) \tag{5.95}$$

where $F(u)$ is the inverse transform of $-i/k(\omega)$. Using integral tables we can show that

$$F(u) = -\sqrt{\frac{2\pi}{\mu_0 \epsilon}} \; e^{-\sigma u/(2\epsilon)} \; J_0(\frac{i\sigma u}{2\epsilon}) \theta(u) \tag{5.96}$$

where J_0 is the Bessel function. The electric field is then

$$E(t) = -\frac{1}{\sqrt{\mu_0 \epsilon}} \int_0^{\infty} \; e^{-\sigma u/(2\epsilon)} J_0(\frac{i\sigma u}{2\epsilon}) g(t-u) \; du \tag{5.97}$$

It is important to note that the electric field at a given time depends only on the preceding values of the magnetic field. This is an example of causality. We can also see this as a consequence of a general mathematical fact: assume that functions $a(t)$ and $b(t)$ are related in the frequency domain by $a(\omega) = c(\omega) b(\omega)$. Assume that $c(\omega)$ has no poles in the half plane $Im(\omega) \geq 0$ and that $|c(\omega)| \to 0$ when $|\omega| \to 0$ in that half plane. Then $a(t)$ depends only on

[10] Weidelt, P., The Inverse Problem of Geomagnetic Induction. Z. Geophys., 38, 257-289, 1972.

previous values of $b(t)$. The reader may verify that these assumptions hold in our example.

In geomagnetic applications, we can simplify Eq. 5.97. It is evident that the Bessel function can be replaced by its asymptotic expression yielding

$$E(t) = -\frac{1}{\sqrt{\pi\mu_0\sigma}} \int_0^\infty \frac{g(t-u)}{\sqrt{u}}\, du = -\frac{1}{\sqrt{\pi\mu_0\sigma}} \int_{-\infty}^t \frac{g(u)}{\sqrt{t-u}}\, du \tag{5.98}$$

This result follows also directly from the low-frequency formula Eq. 5.90. When performing the inverse Fourier transform, it is important to select the correct branch of the complex square root.

Although Eq. 5.98 deals with a very simple model, it reveals some general features of the temporal behaviour of the electric field. As already noted, all previous values of the magnetic field affect the present value of the electric field. However, the most recent ones are the most important due to the weighting factor $1/\sqrt{t}$ in the integral. It follows that the time derivative of the magnetic field is a reasonable proxy for the electric field.

The plane wave formula 5.98 provides an easy way to estimate the geoelectric field from a given time series of the magnetic field. We assume that the magnetic field varies linearly between successive time steps:

$$B(t) = B_{n-1} + \frac{t - T_{n-1}}{\Delta}\left(B_n - B_{n-1}\right),\, T_{n-1} \le t \le T_n \tag{5.99}$$

where $\Delta = T_n - T_{n-1}$ is the sampling interval. Then the electric field at $t = T_N$ is

$$E(T_N) = \frac{2}{\sqrt{\pi\mu_0\sigma\Delta}}\left(R_{N-1} - R_N - \sqrt{M} b_{N-M}\right) \tag{5.100}$$

where $b_n = B(T_n) - B(T_{n-1})$ and

$$R_N = \sum_{n=N-M+1}^{N} b_n \sqrt{N-n+1} \tag{5.101}$$

Here M is the number of previous time steps to be taken into account. Such an explicit time domain approach is feasible only with a uniform and a two-layer earth. Generally, it is more practical to apply the fast Fourier transform (FFT), also with one- and two-layer models.

Finally, it is important to note that causality works in the reverse direction too. This is expected from the Maxwell equations in which the magnetic and electric fields are in equal position. Even more clearly this equality is seen in the electromagnetic field tensor in the Lorentz covariant formulation. An exercise is to show that the magnetic field depends on the electric field as follows:

$$B(t) = -\sqrt{\frac{\mu_0\sigma}{\pi}} \int_0^\infty \frac{E(t-u)}{\sqrt{u}}\, du \tag{5.102}$$

5.5.2 Geomagnetically induced currents

To finish this chapter, we present a practical consequence of geomagnetic induction, namely geomagnetically induced currents (GIC). First, an overview of a larger context, space weather, is given. Then we present in detail a method to model GIC in a power system, and briefly the basic idea of the GIC modelling of a pipeline.

Space physics background

Geomagnetically induced currents flow in man-made conductor systems during geomagnetic variations. The mechanism is easy to understand by Faraday's law: an electric field is associated with a time-varying magnetic field. This geoelectric field in turn drives currents in all conducting materials, and especially within the earth as well as in technological conductor systems. GIC are most easily observed in wide power grids, pipelines, railways, etc.[11]

GIC is an example of phenomena which are nowadays called as space weather phenomena. According to the widely used definition, space weather refers to conditions on the Sun and in the solar wind, magnetosphere, ionosphere, and thermosphere that can influence the performance and reliability of space-borne and ground-based technological systems and can endanger human health. Adverse conditions in the space environment can cause disruption of satellite operations, communications, navigation, and electric power distribution grids, leading to a variety of sosioeconomic losses. Some criticism to this definition has also been stated, because it emphasizes the negative viewpoint. Furthermore, the best-known space weather phenomena are enjoyable auroral displays.

Some of the adverse effects that phenomena in the near space have on systems and the mechanisms behind the effects are sketched in Fig. 5.4. These include single-event upsets in the spacecraft electronics caused by high energy protons, electron induced spacecraft surface and internal charging leading to discharge currents, solar panel degradation due to particle bombardment, tissue damages due to particle radiation, increased atmospheric drag experienced by low orbit spacecraft, disturbances in HF communication and navigation systems caused by the irregularities in the ionosphere, cosmic ray induced neutron radiation at airline hights, GIC in long conductor systems on the ground caused by rapidly varying ionospheric currents, and lastly one of the hottest topics in geophysics, the possible modulation of the neutral atmospheric weather by space weather.

[11] The general description of space weather given here is modified from the introduction of the Ph.D. thesis by Antti Pulkkinen (FMI, 2003). The introduction part is available on WWW at e-thesis: http://ethesis.helsinki.fi/julkaisut/mat/fysik/vk/pulkkinen/

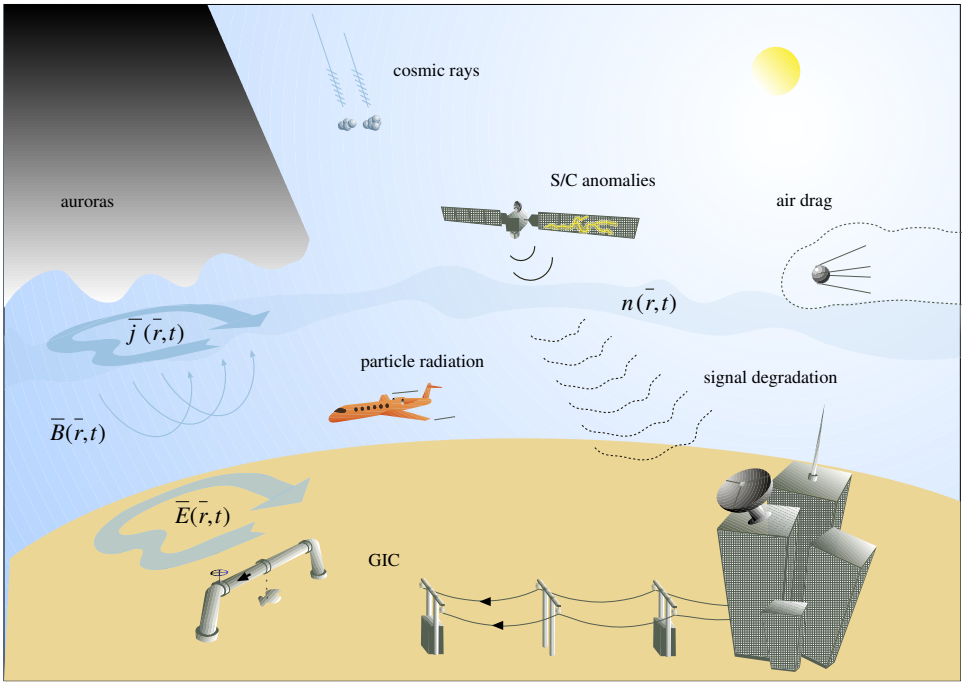

Figure 5.4: Space weather phenomena (figure by Antti Pulkkinen).

GIC can be considered as the last step in the chain of physical connections starting from the Sun (Fig. 5.5):

1. Plasma processes in the Sun cause ejection of material that has the capability of driving geomagnetic activity. From the viewpoint of the strongest ground effects, coronal mass ejections (CME) and coronal holes with high speed solar wind streams are the two most important categories.

2. The propagation of the magnetized plasma structures in the interplanetary medium. From the space weather viewpoint, it is noteworthy that due to absence of remote sensing techniques, the evolution of the structures is very difficult to estimate.

3. Interaction between the solar wind (or structures within) and the magnetosphere. Here the dominant factor for determining the geoeffectiveness of the structure is the orientation of the solar wind magnetic field. The energy feed into the magnetosphere is highest during a strong reconnection of the solar wind and the magnetospheric magnetic fields. An increased energy input to the system sets the conditions for dynamics changes in the magnetospheric electric current systems. One of the manifestations are magnetic storms which are characterized by an enhanced convection of the magnetospheric plasma and an enhanced ring current circulating the Earth.

4. Magnetosphere-ionosphere interaction. The closure of the magneto-

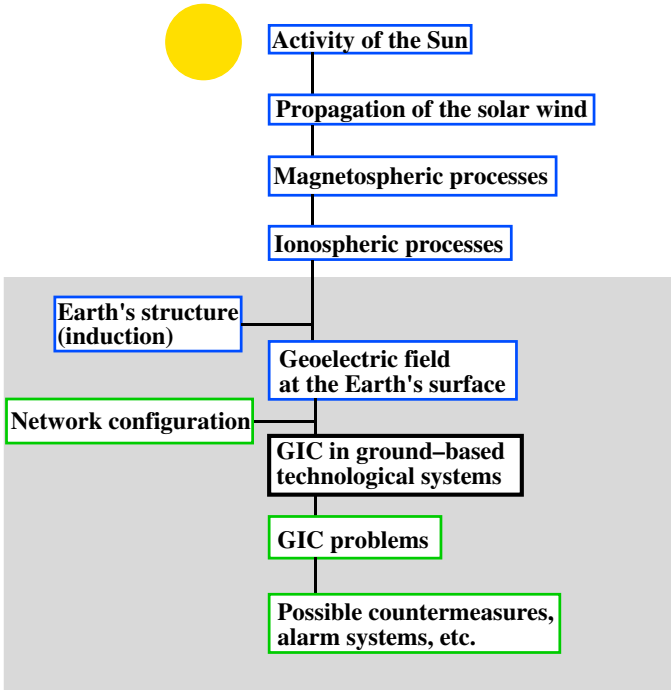

Figure 5.5: Schematic steps of GIC investigations.

spheric currents systems goes via the polar regions of the ionosphere. Correspondingly, dynamic changes in the magnetospheric current systems couple to the dynamics of the ionosphere. An important class of dynamic variations are auroral substorms which are related to loading-unloading processes in the tail of the magnetosphere. During auroral substorms particles injected from the tail are seen in the ionosphere in terms of auroras and rapid changes in the auroral current systems. Although some of the basic features are understood, the details of the storm and substorm processes as well as the storm/substorm relationship are one of the most fundamental open questions in the solar-terrestrial physics.

5. Rapid changes of the ionospheric and magnetospheric electric currents cause variations in the geomagnetic field which according to Faraday's law of induction induce an electric field driving an electric current inside the earth. The nature of this geoelectric field depends on the characteristics of the ionospheric-magnetospheric source and on the earth's conductivity structure. As a rule of thumb, the magnitude of the geoelectric field increases with increasing time derivatives of the ground magnetic field and with decreasing ground conductivity (cf. Sect. 5.5.1).

6. Finally, the geoelectric field drives currents within conductors at and below the earth's surface. The magnitude and distribution of the currents

depend on the topology and electrical characteristics of the system under investigation.

The first technological impacts of space weather were seen on telegraph systems which experienced disturbances in signals and even fires at telegraph stations. However, in principle all conductors can be influenced by GIC. Due to the relatively small magnitudes of geoelectric fields, with maximum observed values being of the order of 10 V/km, only spatially extended systems can be affected.

Operators of the first telegraph systems in the 1830's and 1840's noticed that from time to time there were electric disturbances driving such large anomalous currents in the system that the transmissions of the messages was extremely difficult while at other times no battery was needed for the operation. For example, the famous September 1859 geomagnetic storm produced widespread disturbances in the telegraph systems in North America and Europe. The disturbances coincided with solar flare observations and auroral observations all over the world, and led to speculations about the possible connection between these phenomena. However, the physical explanation remained unclear for the next half century.

After the telegraph equipment, the next category of technological conductor systems affected were power transmission systems, the first known event occurring in 1940[12]. Regarding economic impacts, industrial interests and the number of studies carried out, the effects on power transmission systems are, to the present knowledge, the most important category of space weather effects on the ground. Solely the impact of the March 1989 storm on power systems in North America was greater than reported in other systems altogether at all times.

In power transmission systems, the primary effect of GIC is the halfcycle saturation of high-voltage power transformers. The typical frequency range of GIC is 1–0.001 Hz (periods 1–1000 s), thus being essentially direct current (dc) for the power transmission systems operating at 50 Hz (Europe) and 60 Hz (North America). (Quasi-)dc GIC causes the normally small exciting current of the transformer to increase even to a couple of orders of magnitude higher values, i.e. the transformer starts to operate well beyond the design limits. The saturated transformer causes an increase of the reactive power consumed by the transmission system, ac character of the power transmission which means that the real power available in the system is decreasing. Another effect of the saturated transformer is that the 50 or 60 Hz waveform is distorted, i.e. the higher harmonic content in the electricity increases. Harmonics introduced to the system decrease the general quality of the electricity, and may cause false trippings of protective relays designed

[12] Davidson, W.H., The magnetic storm of March 24, 1940 - effects in the power system, Edison Electric Institute Bulletin, July 1940, 365.

to switch the equipment off in the case of an erratic behaviour. Trippings of the static VAR compensators (employed to deal with the changing reactive power consumption) started the avalanche that finally led to the collapse of the Canadian Hydro-Quebec system on March 13, 1989.

Also more advanced telecommunication cables than single-wire telegraph systems have been affected. The principal mode of failure for these systems is via an erroneous action of the power apparatus that are used for energizing the repeaters of the cable. This is why even modern optic fiber cables could be susceptible to GIC. The best known incidents are the disruption of communications made via TAT-1, the cross-Atlantic (from Newfoundland to Scotland) communication cable in February 1958 and the shutdown of the AT&T L4 cable running in the mid-western US in August 1972. In addition to communication problems in February 1958, there was a blackout in the Toronto area due to a power system failure.

Effects of GIC on pipelines have been of concern since the construction of the Trans-Alaskan pipeline in the 1970's. The flow of GIC along the pipeline is not hazardous but the accompanying pipe-to-soil (P/S) voltage can be a source for two different types of adverse effects. The more harmful one is related to the currents driven by the P/S voltage variations. If the coating, used to insulate the pipeline steel from the soil, has been damaged or the cathodic protection potential used to prevent the corrosion current is exceeded by the P/S voltage, the corrosion rate of the pipeline may increase. However, estimates about the time that it takes from geomagnetic disturbances to seriously corrode pipelines vary quite a lot and no publicly reported failures due to GIC-induced corrosion exist. Thus if the pipeline is properly protected against the corrosion, it is likely that more common effects of GIC are the problems in measuring the cathodic protection parameters and making control surveys during geomagnetic disturbances.

Although railway systems also have long electrical conductors, it seems that malfunctions due to geomagnetic disturbances are very rare. The only reported incident is from Sweden, where during a magnetic storm in July 1982 traffic lights turned unintendedly red. The erroneous operation was explained by the geomagnetically induced voltage that had annulled the normal voltage, which should only be short-circuited when a train is approaching leading to a relay tripping. It is possible that some of past unexplained railway disturbances have in fact been caused by GIC.

In general, GIC has been a source for problems in technological systems on the ground since the mid of the 19th century, the number of reports being roughly a function of the sunspot number and the global geomagnetic activity. The number of technological conductor systems is inevitably increasing and some of these systems will be built in regions where they can be affected by GIC. Thus, GIC may be of concern for system operators also

in the future.

Studies in Finland

GIC studies in Finland started in the end of 1970's as a co-operation between FMI and two industrial partners: Imatran Voima (nowadays Fingrid, owning the high-voltage power system), and Neste/Maakaasu (nowadays Gasum, owning the natural gas pipeline system). The work has included measurements and theoretical modelling and several separate projects have been carried out. The Finnish power system has not suffered from GIC damages, and the same is true for the pipeline too.

The largest GIC measured in the Finnish high-voltage power system was 200 A in the earthing wire of the Rauma 400 kV transformer on March 24, 1991. Due to several changes in the power system and in single transformers, GIC values from different years are not directly comparable. During the latest years, the top GIC values have been some tens of amperes. However, model calculations indicate that 100 A may have been exceeded at some sites (where measurements are not performed).

GIC in the Finnish natural gas pipeline has been measured nearly continuously since November 1998 at the Mäntsälä compresssor station. The recordings are based on the use of two magnetometers: one just above the pipeline and another at the Nurmijärvi Geophysical Observatory about 30 km westward from Mäntsälä. The reader should consider how GIC can be calculated with such an arrangement and what error sources may exist. GIC reached its highest value (57 A) during the October 2003 magnetic storm (Fig. 5.6). As a part of the space weather pilot project of the European Space Agency, FMI maintains a nowcasting service for Gasum[13].

General modelling approach

Calculation of GIC in a given condutor system is convenient to divide into two steps:
1. Determine the geoelectric field associated with geomagnetic variations. This is a purely geophysical problem, which is independent of the technological system.
2. Determine GIC due to the given geoelectric field in a conductor system whose topology and resistances are known.
To justify exactly the division of the problem into these two separate parts is not an easy task. However, it has been discussed thoroughly concerning both power systems and buried pipelines by Pulkkinen (2003). These

[13] http://aurora.fmi.fi/gic_service/

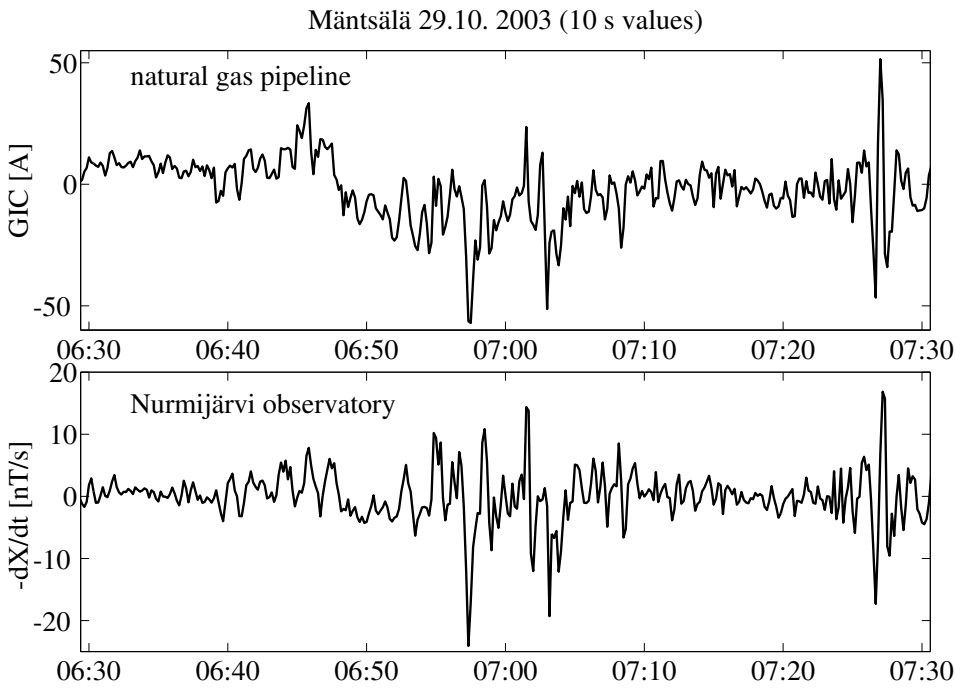

Figure 5.6: The largest GIC event observed at the Mäntsälä compressor station of the Finnish natural gas pipeline on October 29, 2003. The upper panel shows GIC along the pipe (positive eastwards). The lower panel shows the time derivative of the north component of the geomagnetic field at the Nurmijärvi Geophysical Observatory. The time is UT.

theoretical considerations and the long practical experience is convincing to verify the two-step procedure.

In the following we assume that the geoelectric field is known, so we will consider the latter step. A greatly simplifying fact is that geomagnetic variations are slow, so a DC approach is sufficiently accurate for periods longer than about 1 s. In other words, at long periods inductance is ignorable. We will investigate the power system model in detail, and give general guide lines for the significantly more complicated pipeline model.

Power system model

Consider a power system whose geometry and resistances are known (Fig. 5.7). The task is to determine induced currents I_j and I_{jk} due to the geoelectric field $\mathbf{E}$ [14].

[14] Lehtinen, M. and R. Pirjola, Currents produced in earthed conductor networks by geomagnetically-induced electric fields, Ann. Geophys., 3, 479-484, 1985.

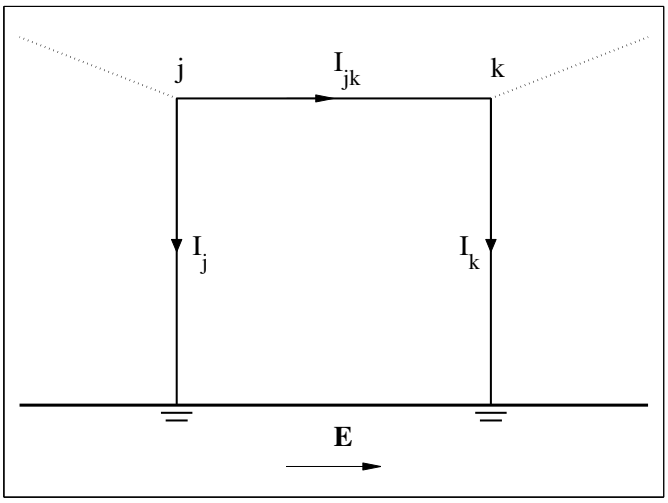

Figure 5.7: Schematic description of a power system.

The voltage between two nodes j and k is defined as the line integral along the power line

$$V_{jk} = \int_j^k \mathbf{E} \cdot \mathbf{dl} \tag{5.103}$$

Define the earthing impedance matrix Z so that the product of Z and the earthing current vector $\mathbf{I} = (I_1, ..., I_N)^T$ yields the voltages U_i between nodes i and the distant earth:

$$U_i = (Z\mathbf{I})_i \tag{5.104}$$

In the static case, the matrix Z is real. If the earthing points are far away from each other Z is also diagonal: $Z_{ij} = R_{ij}\delta_{ij}$. There are some special transformer constructions where non-diagonal elements of Z come into question. However, we will not consider them here.

Since we neglect time-dependence, application of Faraday's law implies

$$\oint \mathbf{E} \cdot \mathbf{ds} = R_{jk}I_{jk} + U_k - U_j - V_{jk} = 0 \tag{5.105}$$

It follows from Kirchhoff's law that

$$I_j = \sum_{k \neq j} I_{kj} = -\sum_{k \neq j} I_{jk} \tag{5.106}$$

The two previous equations yield the earthing current

$$I_j = -\sum_{k \neq j} (V_{jk} + U_j - U_k)/R_{jk} \tag{5.107}$$

Convenient matrix formulas are obtained by defining the admittance matrix Y

$$\begin{aligned} Y_{ij} &= -1/R_{ij}\,,\ i \neq j \\ Y_{ij} &= \sum_{k \neq i} 1/R_{ik}\,,\ i = j \end{aligned} \tag{5.108}$$

Note that $R_{ij} = \infty$ if nodes i and j are not directly connected by a wire. If we also denote

$$\mathbf{J} = (J_1, ..., J_N);\ J_i = \sum_{m \neq i} \frac{V_{mi}}{R_{im}} = -\sum_{m \neq i} \frac{V_{im}}{R_{im}} \tag{5.109}$$

then the earthing current vector $\mathbf{I}$ is obtained from

$$\mathbf{I} = (1 + YZ)^{-1}\mathbf{J} \tag{5.110}$$

Currents along transmission lines are

$$I_{jk} = V_{jk}/R_{jk} + ((Z\mathbf{I})_j - (Z\mathbf{I})_k)/R_{jk} \tag{5.111}$$

A reasonable estimation of GIC is obtained by assuming that the electric field is spatially uniform. In this special case, V_{jk} does not depend on the integration path between nodes j and k. Then the current at a transformer earthing or along a transmission line is

$$GIC(t) = aE_x(t) + bE_y(t) \tag{5.112}$$

where a and b depend only on the geometry and resistances of the network. Typical power grid resistances in Finland vary from 0.1 Ω to a few Ω depending on lengths or lines, local conductivity of the earth and transformer design. The geoelectric field can be up to about 1 V/km during magnetic storms, and GIC may exceed 100 A.

The assumption of a spatially uniform electric field does not usually hold in Finland. An improvement is to derive ionospheric equivalent currents from ground magnetic measurements, as mentioned in Sect. 5.3. Using the complex image method, it is possible to derive closed-form expressions for the electric field in the frequency domain (Sect. 5.3.1). An example of the resulting electric field in the time domain is shown in Fig. 5.8. A strong spatial dependence is evident as well as fast temporal variations.

Another challenge is the horizontal variation of the earth's conductivity. This destroys the assumption of a uniform electric field even in the case of a plane wave primary field. There are detailed models of the conductivity available, but the calculation of the electric field is much slower than with layered earth models.

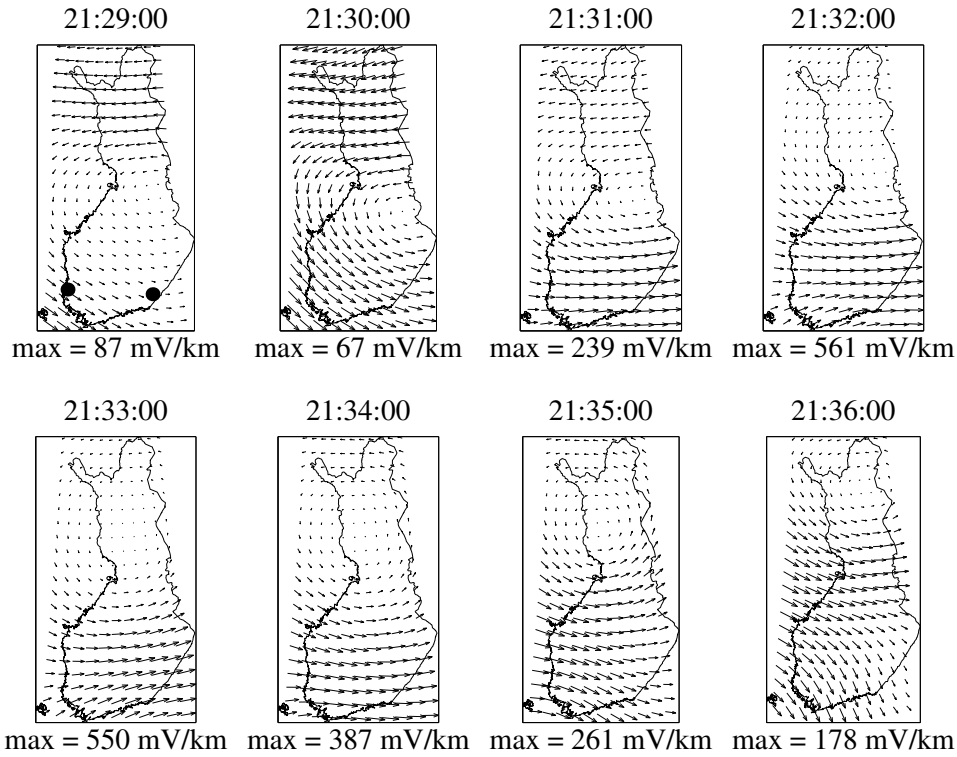

Figure 5.8: The calculated horizontal electric field in Finland on April 11, 2001. The model input were the interpolated magnetic field at the earth's surface and a layered model of the ground conductivity. The leftmost black dot in the first panel shows the location of the Rauma 400 kV transformer.

It may sound that the problem to calculate GIC efficiently does not yet have a proper solution. However, GIC is not sensitive to small-scale variations of the electric field. This is due to the fact that GIC is basically dependent on voltages between nodes. Because transformers in Finland are typically at distances of at least several tens of kilometres, it is sufficient to have a regional conductivity model of such horizontal scales. The present method used in GIC modelling is to determine ionospheric equivalent currents from the recorded ground magnetic field and assume a layered earth model for each site separately. Then the plane wave model is applied locally[15]. Comparison between modelled and measured GIC has shown that this technique works quite well with relative errors of about 30 %. An example of a modelled event is shown in Fig. 5.9.

[15] Viljanen, A., A. Pulkkinen, O. Amm, R. Pirjola, T. Korja, and BEAR Working Group, Fast computation of the geoelectric field using the method of elementary current systems and planar Earth models. Ann. Geophys., 22, 101-113, 2004.

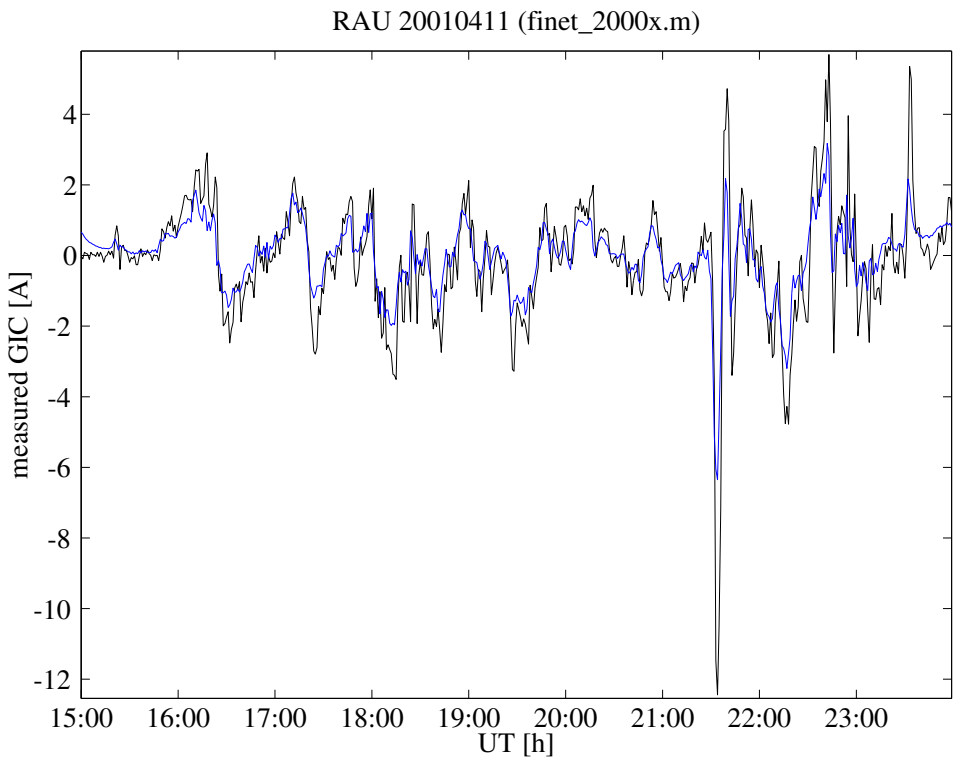

Figure 5.9: The measured (black) and calculated (blue) GIC at the Rauma 400 kV transformer station on April 11, 2001. The measured values were provided by Fingrid. The magnetic field used as input was recorded at the Nurmijärvi Geophysical Observatory. The reader should think about how to improve the fit by modifying the earth's conductivity model.

Pipeline model

Although the basic mechanism of GIC in a buried conductor is the same as for a power system, its mathematical modelling is more challenging. A practical solution to this problem applies transmission line analogy[16,17] . The idea is to construct the pipeline system of straight sections represented by a series impedance Z and a parallel admittance Y, with an external electric field E generating a voltage U (Fig. 5.10).

We can use the transmission line equations in the DC case. The resistance in the section of length dx is Zdx. Applying Ohm's law we obtain

$$IZdx + dV = U = Edx \tag{5.113}$$

[16]Boteler, D. and M.J. Cookson, 1986: Telluric currents and their effects on pipelines in the Cook Strait region of New Zealand. Material Performance, March 1986, 27-32-755.

[17]Pulkkinen, A., R. Pirjola, D. Boteler, A. Viljanen and I. Yegorov, Modelling of space weather effects on pipelines. J. Appl. Geophys., 48, 233-256, 2001.

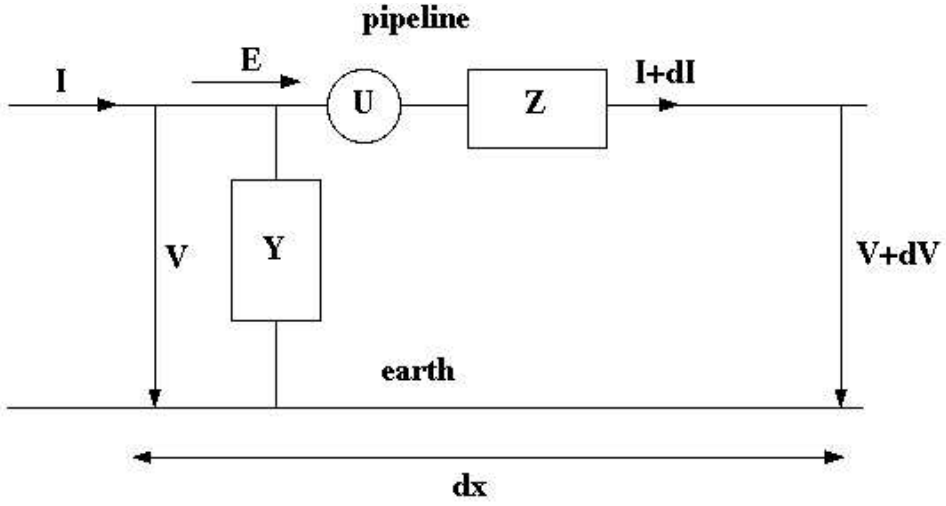

Figure 5.10: A short pipeline section described by the transmission line formulation. The pipe is modelled by an electric circuit characterized by a series impedance Z, a parallel admittance Y and a series voltage source U due to an external electric field E parallel to the pipe.

and similarly

$$VYdx + dI = 0 \tag{5.114}$$

where V is the voltage between the pipe and the earth. It follows that

$$\begin{aligned} \frac{dV}{dx} + ZI &= E \\ \frac{dI}{dx} + YV &= 0 \end{aligned} \tag{5.115}$$

Differentiation and substitution lead to

$$\begin{aligned} \frac{d^2V}{dx^2} - \gamma^2 V &= \frac{dE}{dx} \\ \frac{d^2I}{dx^2} - \gamma^2 I &= -YE \end{aligned} \tag{5.116}$$

where $\gamma = \sqrt{ZY}$ is the propagation constant.

We will only consider one straight section from $x = 0$ to $x = L$ affected by a uniform electric field $\mathbf{E} = E\mathbf{e}_x$. The solution of the transmission line equations is then

$$\begin{aligned} V &= \frac{E}{\gamma}(Ae^{-\gamma x} - Be^{-\gamma(L-x)}) \\ I &= \frac{E}{\gamma Z_0}(1 + Ae^{-\gamma x} + Be^{-\gamma(L-x)}) \end{aligned} \tag{5.117}$$

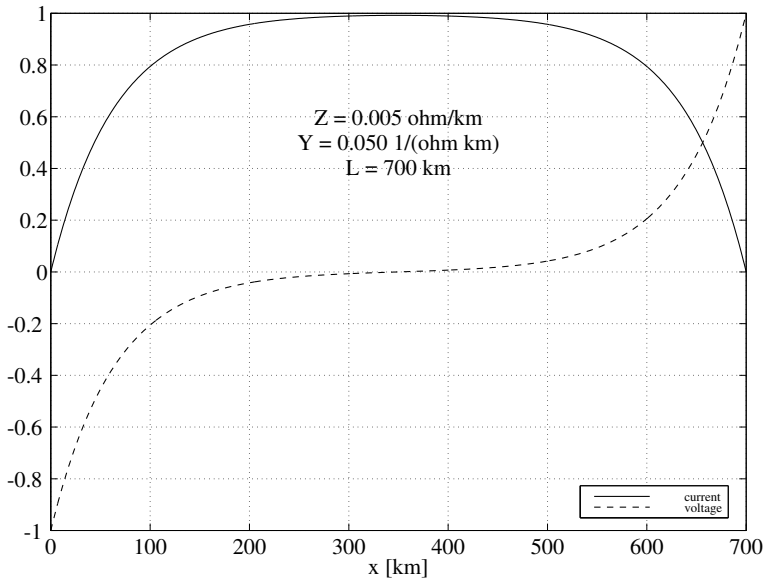

Figure 5.11: Normalized current and voltage in a straight pipe with infinite impedances (zero currents) at ends.

where A and B are constants dependent on the conditions at the ends, and $Z_0 = \sqrt{Z/Y}$ is the characteristic impedance of the pipeline.

As an example, assume that the ends are completely insulated from the ground so that there are no currents there ($I(0) = I(L) = 0$, or in engineering terms, there are infinitely large terminating impedances). Then

$$\begin{aligned} V &= -\frac{E}{\gamma}\frac{e^{-\gamma x} - e^{-\gamma(L-x)}}{1+e^{-\gamma L}} \\ I &= \frac{E}{\gamma Z_0}\frac{1+e^{-\gamma L} - e^{-\gamma x} - e^{-\gamma(L-x)}}{1+e^{-\gamma L}} \end{aligned} \tag{5.118}$$

Figure 5.11 illustrates the current and voltage. An exercise is to consider a very long ($\gamma L \gg 1$) and a very short ($\gamma L \ll 1$) pipe.

The treatment of a general pipeline network containing bends, branches and insulating flanges requires the use of Thevenin's theorem: "Any linear network with two accessible terminals may be replaced by a voltage source acting in series with an impedance. The voltage is that which appears across terminals when they are externally unconnected. The impedance is that viewed at the externally unconnected terminals looking into the network with all independent generators in the network replaced their internal impedances, i.e. open-circuit voltage divided with short-circuit current." We will not study this further here, but just refer to Pulkkinen et al. (2001).

However, a qualitative understanding of more complicated situations is possible based on the results of a straight pipe.